Progress In Electromagnetics Research M, Vol. 11, 137–151, 2010

PATTERN OPTIMIZATION IN AN UWB SPIRAL ARRAY ANTENNA

A. Jafargholi and M. Kamyab

Department of Electrical Engineering
K. N. Toosi University of Technology
Iran

Abstract—We have proposed a new architecture for an array in which the elements are placed on a spiral curve in order to obtain an ultra wideband (UWB) radiation pattern. In addition, array factor and bandwidth of the proposed spiral array are calculated. Simulated results obtained by SuperNEC and CST software have shown good agreement with the analytic calculations. Although the proposed antenna array is wideband in nature, it lacks desirable efficiency, due to poor front to back ratio (FBR) and sidelobe level (SLL). In this paper, we have chosen three different approaches in order to improve the efficiency of proposed array. First, the effect of length and thickness tapering of elements has been studied. Second, we have used Genetic Algorithm (GA) to optimized pattern shape. Finally, the influence of metamaterial cover on array performance has been investigated. Although the first and second methods improve the radiation pattern, the array bandwidth is reduced. It is shown that the third method improves array directivity and FBR by 5–7 dB and 15–17 dB respectively within the frequency band of operation.

1. INTRODUCTION

In the design procedures of an UWB array antennas three main factors should be highly considered. These parameters are array elements, array architecture and feed networks. Appropriate combinations among these factors will determine the performance of array antenna [1]. Several array elements have been introduced previously in [2, 3]. The array architecture as the second important parameter in array antennas design is determined by desired array bandwidth, radiation pattern and array scan ranges [1]. Furthermore,

Corresponding author: A. Jafargholi (ajafargholi@ee.kntu.ac.ir).

the feed network plays an important role in the performance of the whole system and should be designed based on array elements and array architecture [4, 5]. In [6], UWB spiral array architecture has been introduced, and a desired null over 75 MHz bandwidth from 35 to 110 MHz has been achieved. Although the authors have applied the Genetic Algorithm to achieve the desired pattern, the design procedure as well as array bandwidth and directivity have not been discussed.

In this paper, we investigate a new architecture for an array in which the elements are placed on a spiral curve in order to obtain an UWB directivity and radiation pattern. The array factor and bandwidth of the proposed spiral array architecture have been presented. Although the illustrated array has UWB radiation pattern with broadband directivity characteristic, $D_{\max} = 10\,\text{dBi}$ over 0.5–3.5 GHz, the array SLL and FBR are not acceptable, 5–10 dB, and they degraded to total array efficiency.

To modify the array radiation pattern, we studied three different approaches, including tapering the antenna elements, using Genetic Algorithm (GA) and using metamaterial cover as a reflector. First, the effects of length and thickness tapering on directivity and FBR of spiral array antennas have been investigated. Although this method has good effects on array FBR bandwidth, it is not efficient in directivity enhancement except in small fraction of frequency. GA is the other method to shape the array pattern which is investigated here. Although this method has good effects on array radiation pattern, the strict limitation is applied to the array bandwidth.

Introducing metamaterials structures, novel subjects such as miniaturization of antennas have attracted remarkable attention and they have found their applications in enhancement of directivity of antennas [7, 8]. One solution to this problem is to use metamaterial cover the patch antenna [9–12]. One of the first works was done by Temelkuaran in 2000 [13]. In 2002, Enoch proposed a kind of metamaterial for directive emission [14]. Another problem associated with microstrip antennas is their narrow bandwidth. The previous works so far [10–12] have dealt only with the enhancement of the antenna directivity using metamaterial cover, but the effect of this cover on the antenna input impedance has not been investigated. Recently, a new metamaterial cover has been proposed to enhance both the antenna bandwidth and directivity [15]. But, its directivity is significantly lower compared to the primary metamaterial cover [9–12]. Recently, EBG structures have been used as a reflector [16] and in place of cavity to make a low profile UWB spiral antenna [17]. In this paper, we proposed a metamaterial cover which is simple to realize and easy to fabricate. By applying three types of metamaterial

structures, the array directivity and FBR enhancement, within a frequency range of 0.5–3.5 GHz, have been studied. Simulations show that the modifications are about 5–7 dB, and 15–17 dB for directivity and FBR respectively.

In order to investigate the array directivity and pattern modification, an ordinary monopole element which has UWB radiation pattern has been used without any impedance bandwidth consideration. Although in Sections 3 and 4, the presented simulations are based on this monopole antenna, in Section 5, an UWB antenna element, which is operated above 3.5 GHz, has been suggested.

2. ARRAY ANTENNA FORMULATION

For an m-element simple spiral array antenna, the position vector may be written:

$$\vec{r}_m = \vec{r}e^{a\phi_m} = r_0 e^{a\phi_m} \cos(\phi_m)\,\hat{x} + r_0 e^{a\phi_m} \sin(\phi_m)\,\hat{y} \qquad (1)$$

where a is the spiral constant and specifies the increasing rate of the spiral radius proportionate with angle ϕ_m, $\hat{x}$ and $\hat{y}$ are the unit vectors along the x and y axis respectively, and x_m and y_m are the cartesian location of the array elements and $\vec{r}$ is the vector of spiral constellation. In Fig. 1, r_0 is the distance of the first element of the array from the origin and $\phi_m = \frac{(m-1)\pi}{b}$ represents the angle of mth element in polar coordinate, where parameter b may be chosen arbitrary in order to make smoother change in spiral contour and to increase the degree

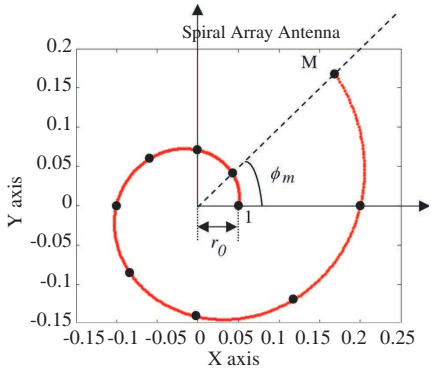

Figure 1. A spiral array architecure which elements locations are spesified by Equation (1) and circles on the spiral contour, first and last elements are specified by 1 and M, $M = 10$, $b = 4$, $f_0 = 3$ GHz, $r_0 = \lambda/2$, $a = 0.221$.

of freedom in design. It should be noted that b has a positive value ($b > 0$). The array factor of the spiral array is [1]:

$$AF(\theta,\phi) = \sum_{m=1}^{M} I_m e^{j\left(\frac{2\pi}{\lambda} r_0 e^{a\phi_m} \sin\theta\cos(\phi-\phi_m)+\delta_m\right)} \tag{2}$$

Using perturbation theory, the array bandwidth for the proposed structure has been calculated and presented here. Assume that

$$r_0 = d\lambda_0 = d\frac{c}{f_0} \tag{3}$$

And

$$\frac{r_0}{\lambda} = \frac{dc}{f_0}\Big/\frac{c}{f} \Rightarrow \frac{r_0}{\lambda} = \frac{df}{f_0} \tag{4}$$

By substituting $\frac{r_0}{\lambda}$ in (2), we can rewrite the array factor in term of frequency, f, and angle, ϕ_0, as follows:

$$AF(\phi_0,f) = \sum_{m=1}^{M} I_m e^{j\left(\frac{2\pi df}{f_0} e^{a\phi_m} \sin\theta\cos(\phi_0-\phi_m)+\delta_m\right)} \tag{5}$$

Let $\delta_m = 0$, by expanding Equation (5) in terms of frequency, using Taylor expansion regard to f_0 we have:

$$f(x) = f(x_0) + \frac{\partial}{\partial x} f(x)\Big|_{x=x_0} \times (x-x_0) + \ldots$$

where

$$\begin{aligned} f(x) &= \sum_{m=1}^{M} I_m e^{j\frac{2\pi d}{f_0} x e^{a\phi_m} \sin\theta\cos(\phi_0-\phi_m)} \\ \frac{\partial}{\partial x} e^{px} &= p e^{px} \\ p &= j\frac{2\pi d}{f_0} e^{a\phi_m} \sin\theta\cos(\phi_0-\phi_m) \end{aligned}$$

Thus, we have

$$\begin{aligned} AF(\phi_0,f) = &\sum_{m=1}^{M} I_m e^{j2\pi d e^{a\phi_m} \sin\theta\cos(\phi_0-\phi_m)} \\ &+ j\frac{2\pi d}{f_0}(f-f_0)\sin\theta \sum_{m=1}^{M} I_m \begin{bmatrix} e^{a\phi_m}\cos(\phi_0-\phi_m)\cdot \\ e^{j2\pi d e^{a\phi_m} \sin\theta\cos(\phi_0-\phi_m)} \end{bmatrix} \end{aligned} \tag{6}$$

Simplification of (6) leads to

$$AF(\phi_0, f) = \sum_{m=1}^{M} I_m e^{j2\pi d e^{a\phi_m} \sin\theta \cos(\phi_0 - \phi_m)} \times \left\{ 1 + j\frac{2\pi d}{f_0}(f - f_0)\sin\theta \sum_{m=1}^{M} e^{a\phi_m} \cos(\phi_0 - \phi_m) \right\} \quad (7)$$

From (7), the normalized absolute is

$$\left|\overline{AF}(\phi_0, f)\right| \leq 1 + \frac{2\pi d}{f_0} \cdot |f - f_0| \cdot \sum_{m=1}^{M} e^{a\phi_m} \quad (8)$$

Assuming that the main lobe in azimuth axis is located at $\phi = \phi_0$ and the normalized main beam is defined as $|\overline{AF}(\phi_0, f)| \approx 1 - \varepsilon$ where ε is a positive small value, we have

$$1 - \varepsilon|_{\varepsilon \to 0} \cong \left|\overline{AF}(\phi_0, f)\right| \leq 1 + \frac{2\pi d}{f_0} \cdot |f - f_0| \cdot \sum_{m=1}^{M} e^{a\phi_m} \quad (9)$$

And we have

$$\frac{\Delta f}{f_0} = \frac{2|f - f_0|}{f_0} \leq \frac{\varepsilon}{\pi d} \left(\sum_{m=1}^{M} e^{a\phi_m} \right)^{-1} \quad (10)$$

Using (7) and (10), we may express the array 3-dB bandwidth approximately as

$$BW_{3\text{dB}} = \frac{M}{\pi d} f_0 \left(\sum_{m=1}^{M} e^{a\varphi_m} \right)^{-1} \quad (11)$$

We analyzed spiral array architecture within a frequency range of 1–5 GHz. The array has been simulated using SuperNEC and CST Microwave software. The simulation results are in good agreement with analytical results. We have chosen monopole antennas as array elements. In addition, it is assumed that antenna elements impedances are matched over the entire frequency bands. To study the array performance, a 7-element spiral array, with parameters $r_0 = \lambda_C/2$, $a = -0.221$ and $b = 3$, at the central frequency $f_c = 3$ GHz and $\lambda_C = 5$ cm has been analyzed theoretically. Using Equation (1), the elements locations are specified in Table 1. According to progressive phase excitation method and uniform amplitude, for the main lobe located at (θ_0, ϕ_0), the phase δ_m for each element can be expressed as [1]:

$$\delta_m = -\frac{2\pi}{\lambda} r_0 e^{a\phi_m} \sin\theta_0 \cos(\phi_0 - \phi_m) \quad (12)$$

Table 1. Spiral array elements properties for 1–5 GHz.

Elements No.	1	2	3	4	5	6	7
Location, (x) (cm)	5.0	1.98	−1.57	−2.49	−0.99	0.78	1.25
Location, (y) (cm)	0	3.44	2.73	0	−1.72	−1.36	0
Current	1.0	−0.54 −0.82i	−0.14 −.99i	1.0	−0.47 +0.88i	0.65 +0.75i	1.0

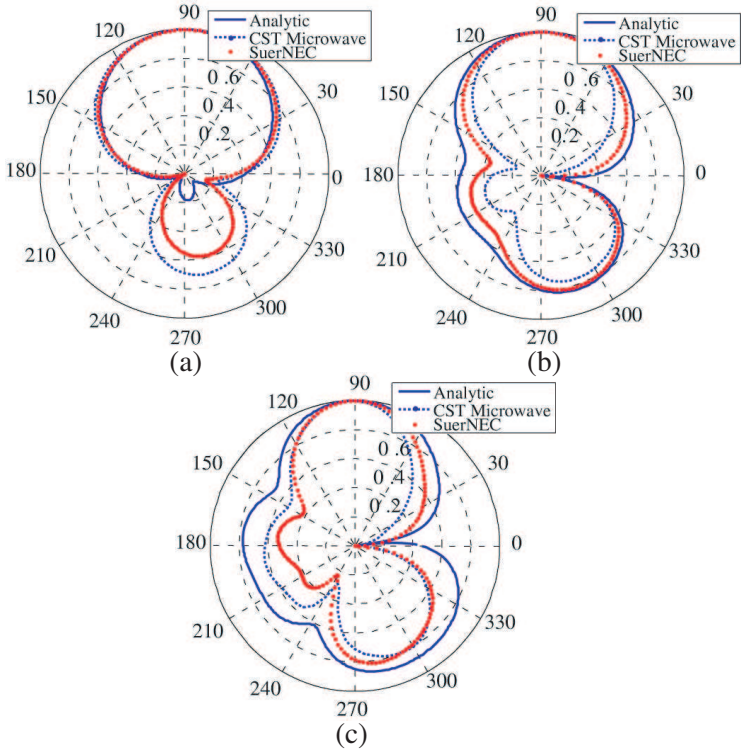

Figure 2. Analytic, SuperNEC and CST simulation results for array radiation pattern in azimuth plane, $\theta = 90°$, (antenna length = 12.5 mm) at (a) 2 GHz, (b) 3 GHz, (c) 4 GHz.

The arrays have been designed for the main lobe location in $(\theta_0, \phi_0) = (90, 90)$ and the feeding values of these elements are also specified in Table 1.

The theoretically results for $f = 2$, 3, and 4 GHz are shown in Fig. 2. To simulate the structure with the aid of the mentioned software the array elements are located on infinite perfect ground. On Fig. 2, calculated results are compared with those obtained through simulations, which show a very close agreement. It is noted that unlike ordinary arrays, the main direction of radiation pattern does not change versus frequency.

The numerical simulations show that for the proposed spiral array, Table 1, the center frequency and array bandwidth are $f_0 = 3.35$ GHz and 3.7 GHz (1.5 to 5.2 GHz) respectively. Using (11), and substituting $a = -0.221$, $M = 7$ and $d = 0.5$, the array fractional bandwidth, Δf, which is about $\Delta f = 1.092$, lead to $\Delta f \times f_0 = 3.66$ GHz for array 3-dB bandwidth, while it is shown good agreement with results obtained by numerical simulations.

3. ARRAY TAPERING

Although illustrated array has UWB radiation pattern with broadband directivity characteristic, the array FBR is not acceptable and it has adverse the effects on the array efficiency. Thus, we used some tapering techniques to resolve thi problem. In order to show the positive effect of tapering, we expand the frequency band to 6 GHz. Also, we divide our analysis into four sections. In the first section, no tapering is applied to the length and thickness of array elements. At this case, the length and thickness of all array elements are 12.5 and 1 mm, respectively. In the second section, the length of array elements, i.e., monopole antennas, is tapered. At the case in hand, the length of elements is gradually increased from 7.5 to 22.5 mm. In the third section, the lengths of elements are left constant, i.e., 12.5 mm, and the thickness of array elements are gradually increased from 0.5 to 2 mm. Finally, the length and thickness of array elements have been tapered simultaneously. At this case, the length and thickness of array elements are gradually increased in the range of 7.5–22.5 mm and 0.5–2.0 mm, respectively. The length and thickness of array elements are summarized in Table 2.

The maximum directivity for aformentioned spiral array is plotted against frequency and is shown in Fig. 3(a). As we can see in this figure, the effect of tapering on the maximum directivity of spiral array is not considerable, especially in the lower frequencies. In contrast to the array directivity, the effect of tapering on FBR is considerable but in

small fraction of frequency the FBR is dropped which could be ignored. Fig. 3(b) shows that if the length and thickness of array elements are tapered simultaneously, the FBR of array is improved up to 10 dB. In general, the tapering improves FBR in comparison with no-tapering situation.

Table 2. Length and thickness of tapered elements (a) tapered length, (b) tapered thickness, (c) tapered both thickness and length.

Elements No.	1	2	3	4	5	6	7
Length (mm)	7.5	10	12.5	15	17.5	20	22.5
Thickness (mm)	2	2	2	2	2	2	2

(a)

Elements No.	1	2	3	4	5	6	7
Length (mm)	12.5	12.5	12.5	12.5	12.5	12.5	12.5
Thickness (mm)	0.5	0.75	1	1.25	1.5	1.75	2

(b)

Elements No.	1	2	3	4	5	6	7
Length (mm)	7.5	10	12.5	15	17.5	20	22.5
Thickness (mm)	0.5	0.75	1	1.25	1.5	1.75	2

(c)

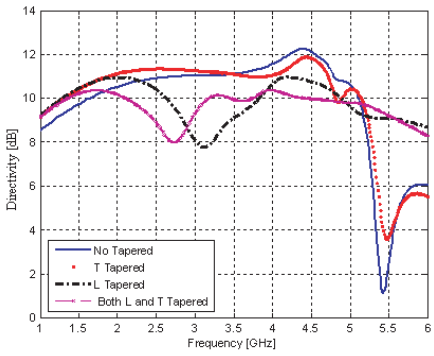

(a)

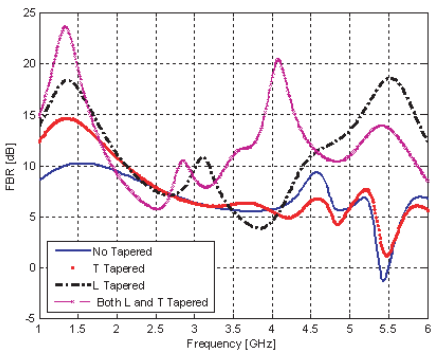

(b)

Figure 3. (a) The maximum directivity and (b) FBR of tapered spiral arrays v.s. frequency.

4. SHAPING THE ARRAY RADIATION PATTERN USING GENETIC ALGORITHM METHOD

Now, we proposed the results of pattern shaping using GA and its effects on array bandwidth. It is well known that the GA method is a strong optimization method which helps to find the global min/max point of a considered problem. So it is expect that using such method and applying it to find the minimum SLL and maximum FBR, may corrupt the array bandwidth. On Fig. 4, the simulation result of GA optimization for predefined spiral array (Table 1) for $f = 3\,\text{GHz}$ and SLL $= 15\,\text{dB}$ is presented. By defining such desired pattern and without strictness on array beamwidth, the array bandwidth is defined over 1.2–3.3 GHz (2.75 : 1). It is noted that unlike previous suggestion, the arrays bandwidth is limited. In Table 3, the feeding values of these elements are specified.

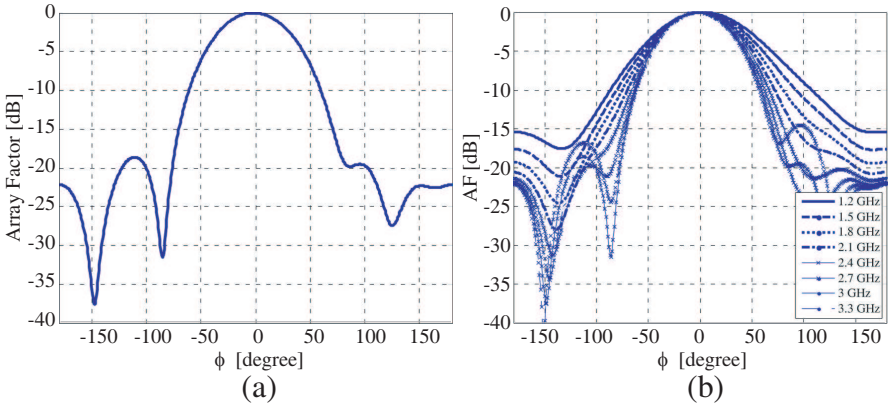

Figure 4. The array radiation patern (a) optimizied by GA, (b) variation v.s. frequency.

Table 3. GA results for spiral array elements 1.2–3.3 GHz.

Elements No.	1	2	3	4	5	6	7
Current	0.04	−0.148	0.28	−0.178	0.51	−0.35	0.059

Table 4. Antenna element and metamaterial cover parameters.

Length (mm)	Γ	D	H	L	Thickness	R	Ha	Hb
	15	10	75	150	2.5	10	5	10

5. ENHANCEMENT OF DIRECTIVITY AND FRONT TO BACK RATIO USING METAMATERIAL COVER STRUCTURES

It is time to investigate a new application of metamaterial cover to realize an UWB reflector with modified characteristics versus traditional PEC reflectors. First, it is assumed that a metamaterial cover is placed at the back of the spiral array (opposite direction of array main lobe-it should be noted that in this method the structure could be used in fixed beam array, neither in scan array and nor in phase array).

In order to direct the antenna radiation pattern, we consider three types of metamaterial structures, which are placed as it shown in Fig. 5(a). The structures include a PEC sheet with hollow periodic squares, circles and hexagonal which placed behind the spiral array and act as a metamaterial reflector. The unit cell of metamaterial structures are depicted in Fig. 5(b). The height, length, and thickness of metamaterial cover sheets are 75, 150, and 2.5 mm, respectively. The parameters of an UWB antenna element are presented in Fig. 5(c) and Table 4, respectively. The effects of a sheet of metamaterial structure on maximum directivity and FBR of aforementioned spiral array have been shown in Fig. 6.

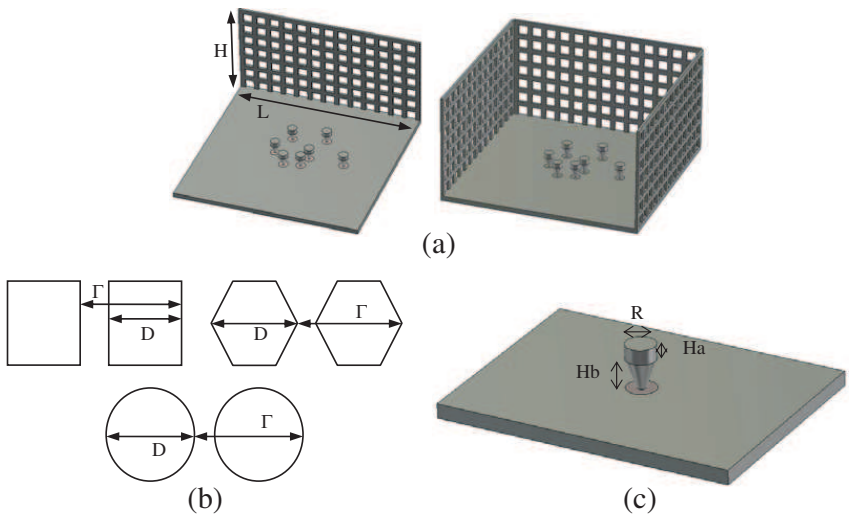

Figure 5. (a) Configuration of the array antenna with single and triple, square-metamaterial cover, (b) the unit cell of rectangular-, circlular-, and hexagonal- metamaterial cover, and (c) UWB antenna element.

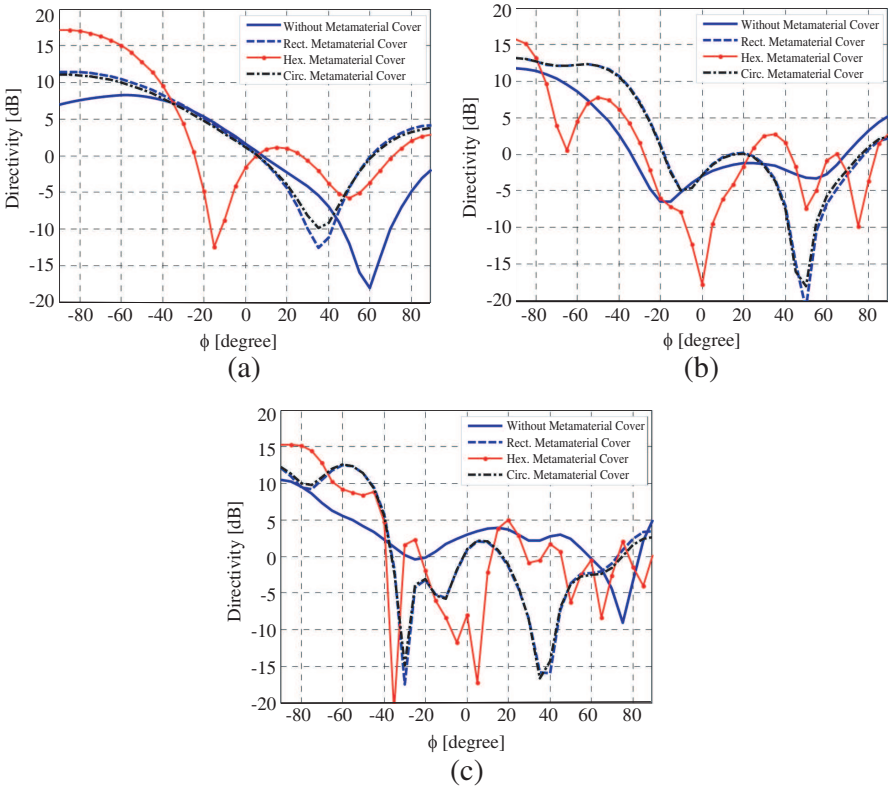

Figure 6. The directivity patterns (At $\theta = 90°$) of designed spiral array which is surrounded by one rectangular, circular or hexagonal metamaterial cover at (a) 1 GHz, (b) 3 GHz, (c) 5 GHz.

The effect of hexagonal metamaterial on the maximum directivity is similar to the reflector at the frequency range from 1 to 3.0 GHz. But the maximum directivity and FBR can be considerably improved by using hex-metamaterial covers. Also, the hex-metamaterial structure has the best performance between the metamaterial covers shown in Fig. 5(b). In triple sheets of metamaterial structure, the results have some different with previous, Fig. 7.

Although the hex-metamaterial structure modifies the array characteristics, it is clear that the rectangular metamaterial structure has best performance between suggested structures and it could provide wider frequency range in comparison with others. The normalized radiation pattern of the mentioned spiral array antenna obtained by CTS Microwave is shown in Fig. 8.

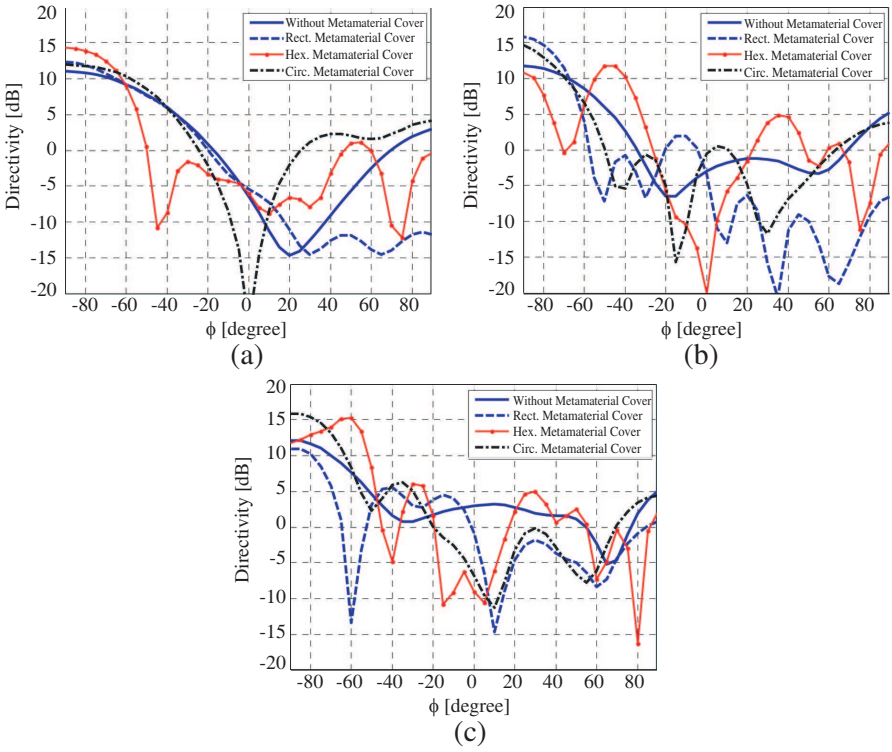

Figure 7. The directivity patterns (At $\theta = 90°$) of designed spiral array which is surrounded by three rectangular, circular or hexagonal metamaterial cover at (a) 1 GHz, (b) 3 GHz, (c) 5 GHz.

The antenna return loss in four conditions is compared in Fig. 9. The results show that the antenna return loss has been modified when a metamaterial cover has been used. Moreover, for single and triple sheets of metamaterial cover, no significant difference has been specified.

Using larger elements cause lower frequency band; however it cause degradation in array radiation pattern due to increasing the mutual coupling effects. Moreover, decreasing distance between the antennas elements cause degradation in position on the spiral constellation which it leads to more undesirable effects on array characteristics. These limitations lead to an UWB element which is matched over 3–5 GHz and omnidirectional radiation characteristics.

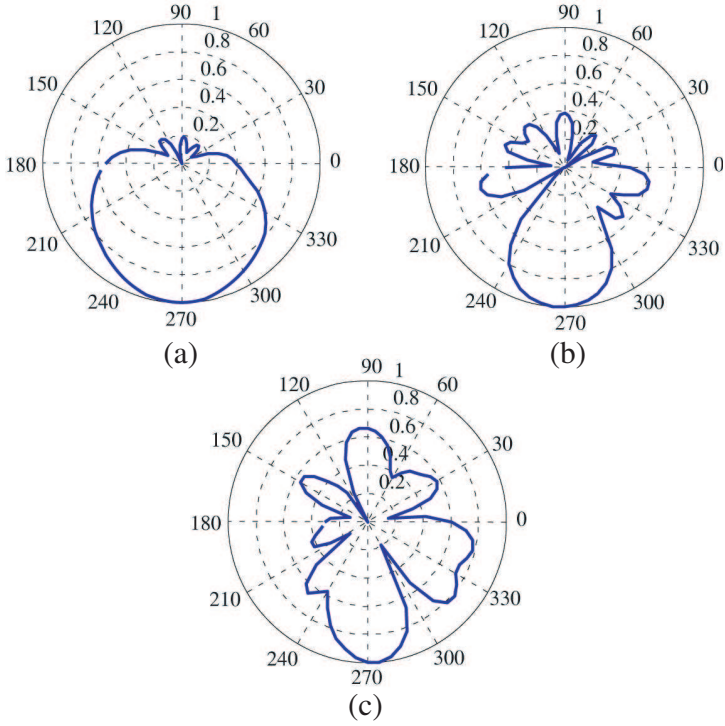

Figure 8. Normalized radiation patterns (At $\theta = 90°$ and in polar coordinate) of designed spiral array which is surrounded by three sheets of rectangular metamaterial cover at (a) 1 GHz, (b) 3 GHz, (c) 5 GHz.

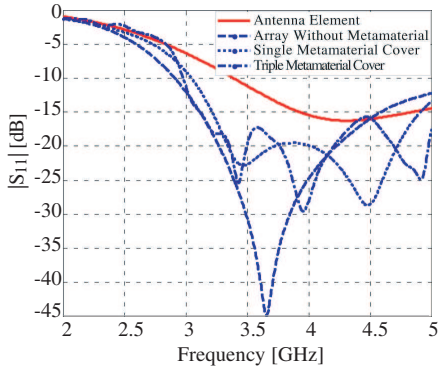

Figure 9. Return loss of antenna element and designed spiral array which is surrounded by a sheet or three sheets of rectangular metamaterial cover.

6. CONCLUSION

In this paper, we studied the effect of tapering technique on the array directivity and FBR of the proposed spiral array antennas. We also suggest using GA method to shape the radiation pattern through array frequency bandwidth. Furthermore, we proposed three types of metamaterial structure to enhance the array performance. The simulation results show that if we enclose the array antenna with three rectangular metamaterial cover, the maximum directivity and FBR of spiral array antenna will be improved considerably. Also, we can deduce that the proposed structure can be used for realization of high-directive UWB spiral array antennas. It should be noted that in the last method the enhancement could be used only in fixed array pattern, not in scan array and nor in phased array antennas.

REFERENCES

1. Allen, B., M. Dohler, E. E. Okon, W. Q. Malik, A. K. Brown, and D. J. Edwards, *Ultra-wideband Antennas and Propagation for Communications, Radar and Imaging*, John Wiley, New York, 2007.
2. Rajagopalan, A., G. Gupta, A. S. Konanur, B. Hughes, and G. Lazzi, "Increasing channel capacity of an ultrawideband MIMO system using vector antennas," *IEEE Trans. Antennas Propag.*, Vol. 55, No. 10, 2880–2887, Oct. 2007.
3. Ren, Y.-J. and K. Chang, "An ultrawideband microstrip dual ring antenna for millimeter-wave applications," *IEEE Trans. Antennas Propag.*, Vol. 6, 457–459, 2007.
4. Panduro, M. A. and C. del Rio Bocio, "Design of beam-forming networks for scannable multi-beam antenna arrays using corps," *Progress In Electromagnetics Research*, PIER 84, 173–188, 2008.
5. Emadi, M., K. H. Sadeghi, A. Jafargholi, and F. Marvasti, "Co channel interference cancellation by the use of iterative digital beamforming method," *Progress In Electromagnetics Research*, PIER 87, 89–103, 2008.
6. Jafargholi, A., M. Mousavi, M. Emadi, and M. Nayebi, "Wide-band nulling by five elements spiral array antenna," *6-th International Conference on ITS Telecommunications*, 446–448, 2006.
7. Weng, Z.-B., Y.-C. Jiao, G. Zhao, and F.-S. Zhang, "Design and experiment of one dimension and two dimension metamaterial

structures for directive emission," *Progress In Electromagnetics Research*, PIER 70, 199–209, 2007.

8. Liang, L., C. H. Liang, L. Chen, and X. Chen, "A novel broadband EBG using cascaded mushroom-like structure," *Microw. Opt. Technol. Lett.*, Vol. 50, No. 8, 2167–2170, 2008.
9. Alù, A., F. Bilotti, N. Engheta, and L. Vegni, "Metamaterial covers over a small aperture," *IEEE Trans. Antennas Propag.*, Vol. 54, No. 6, 1632–1643, Jun. 2006.
10. Xu, H., Z. Zhao, Y. Lv, C. Du, and X. Luo, "Metamaterial superstrate and electromagnetic band-gap substrate for high directive antenna," *Int. J. Infrared Milli. Waves*, Vol. 29, 493–498, 2008.
11. Zhu, F., Q. Lin, and J. Hu, "A directive patch antenna with a metamaterial cover," *Proceedings of Asia Pacific Microwave Conference*, 2005.
12. Huang, C., Z. Zhao, W. Wang, and X. Luo, "Dual band dual polarization directive patch antennausing rectangular metallic grids metamaterial," *J. Infrared Milli. Terahz Waves*, Vol. 30, 700–708, 2009.
13. Temelkuaran, B., M. Bayindir, E. Ozbay, R. Biswas, M. Sigalas, G. Tuttle, and K. M. Ho, "Photonic crystal-based resonant antenna with a very high directivity," *Journal of Applied Physics*, Vol. 87, 603–605, 2000.
14. Enoch, S., G. Tayeb, P. Sabouroux, N. Guérin, and P. Vincent, "A metamaterial for directive emission," *Physical Review Letters*, Vol. 89, 213902, 2002.
15. Ju, J., D. Kim, W. J. Lee, and J. I. Choi, "Wideband high-gain antenna using metamaterial superstrate with the zero refractive index," *Microw. Opt. Technol. Lett.*, Vol. 51, No. 8, 1973–1976, 2009.
16. Yang, F. and Y. Rahmat-Samii, *Electromagnetic Band Gap Structures in Antenna Engineering*, Cambridge University Press, 2008.
17. Nakano, H., K. Kikkawa, N. Kondo, Y. Iitsuka, and J. Yamauchi, "Low-profile equiangular spiral antenna backed by an EBG reflector," *IEEE Trans. Antennas Propag.*, Vol. 57, No. 5, 1309–1318, May 2009.